



Published in final edited form as:

Adv Anat Pathol. 2021 July 01; 28(4): 251–257. doi:10.1097/PAP.0000000000000299.

Eosinophilic Vacuolated Tumor of the kidney: a review of evolving concepts in this novel subtype with additional insights from a case with *MTOR* mutation with concomitant chromosome 1 loss

Payal Kapur, MD^{1,2,3}, Ming Gao, PhD^{3,4}, Hua Zhong, PhD^{1,5}, Dinesh Rakheja, MD^{1,3}, Qi Cai, MD¹, Ivan Pedrosa, MD, PhD^{3,6}, Vitaly Margulis, MD^{2,3}, Lin Xu, PhD⁷, Lisa Kinch, PhD⁷, James Brugarolas, MD, PhD^{3,4}

¹Department / Center of Pathology, University of Texas Southwestern Medical Center, Dallas, TX, 75390

²Department / Center of Urology, University of Texas Southwestern Medical Center, Dallas, TX, 75390

³Department / Center of Kidney Cancer Program at Simmons Comprehensive Cancer Center, University of Texas Southwestern Medical Center, Dallas, TX, 75390

⁴Department / Center of Hematology-Oncology Division of Internal Medicine, University of Texas Southwestern Medical Center, Dallas, TX, 75390

⁵Department / Center of Bioinformatics, University of Texas Southwestern Medical Center, Dallas, TX, 75390

⁶Department / Center of Radiology, University of Texas Southwestern Medical Center, Dallas, TX, 75390

⁷Departments / Centers of Population and Data Sciences, University of Texas Southwestern Medical Center, Dallas, TX, 75390

Abstract

Recent advances in molecular genetics have expanded our knowledge of renal tumors and enabled better classification. These studies have revealed that renal tumors with predominantly “eosinophilic/ oncocyctic” cytoplasm include a number of novel biologic subtypes beyond the traditionally well recognized renal oncocytoma (RO) and eosinophilic variant of chromophobe renal cell carcinoma (ChRCC). Herein, we present a comprehensive review of Eosinophilic Vacuolated Tumor (EVT), a recently described novel renal epithelial tumor subtype. Leveraging the comprehensive study of radiology, histopathology, electron microscopy and next generation sequencing of a patient with EVT with sporadic *MTOR* mutation, we shed insight on the

Author of correspondence: Payal Kapur, MD, Professor, Department of Pathology, University of Texas Southwestern Medical Center, 5323 Harry Hines Blvd., Phone: 214-633-6363, Fax: 214-633-8817, payal.kapur@utsouthwestern.edu & James Brugarolas, MD, PhD, Professor, Department of Internal Medicine, Hematology-Oncology Division, University of Texas Southwestern Medical Center, 5323 Harry Hines Blvd., Phone: 214-648-4059, Fax: 214-648-1960, james.brugarolas@utsouthwestern.edu.

Conflicts of interest disclosures: None

pathogenesis of EVT. These data allows us to postulate that loss of chromosome 1 loss observed in EVT with *MTOR* mutation may be related to mTORC1 being a dimer since a heterodimer of wild-type and mTOR p.L2427R proteins may not confer sufficient mTORC1 activation. mTORC1 is best known for its role in promoting protein translation. Consistently, dilated cisterns of rough endoplasmic reticulum (ER) were noted on electron microscopic examination that likely corresponded to the cytoplasmic vacuoles seen by light microscopy. This ER expansion may contribute to the increase in phospho-S6 observed in these tumors, as S6 is a ribosomal protein and ribosomes may be increased with the ER expansion. We further discuss the evolving concepts in the classification of this emerging entity.

Keywords

Eosinophilic variant of chromophobe renal cell carcinoma; RCC with cytoplasmic eosinophilia; eosinophilic tumor; unclassified oncocytic tumor; hybrid oncocytic/ chromophobe RCCs; Eosinophilic Vacuolated Tumor; high-grade oncocytic tumor; TSC associated RCC; MTOR

Introduction

In the last few years several novel entities have been characterized within the spectrum of “unclassified eosinophilic renal tumors”. These include eosinophilic solid and cystic (ESC) renal cell carcinoma (RCC)^{1,2}, low-grade oncocytic tumor (LOT)³, and high-grade oncocytic tumor (HOT)/ sporadic RCC with eosinophilic and vacuolated cytoplasm⁴⁻⁶. More recently, the term “eosinophilic vacuolated tumor (EVT)” has being proposed for the last entity. Though the initial publication described EVT as a sporadic entity harboring somatically acquired mutations in mTORC1 regulating genes (*TSC2* or *MTOR*), it has now also been described in a Tuberous Sclerosis Complex (TSC) patient⁴. Herein, we present a comprehensive review of this rare and novel entity describing, for the first time, its electron microscopy features and including next-generation whole exome sequencing results.

Case Report

A 55-year-old male was incidentally found to have a small renal mass during workup for ischemic colitis. Computerized tomography (CT) scan of the abdomen revealed a solitary heterogeneous, 1.8 cm exophytic midpole left renal mass without evidence of metastatic disease (Figure 1A). The patient had no prior documented history of TSC or other known hereditary syndromes. He underwent a left partial nephrectomy with negative margins (pT1aNxM0) and he remains well and free of recurrence 15 months post resection.

Gross and Histologic Findings

Gross examination revealed a well circumscribed, solid, tan-brown mass. The tumor was completely submitted and microscopy showed a well-circumscribed, non-encapsulated, solid tumor (Figure 1B). The tumor was composed of nests and sheets of tumor cells in a hypovascular, hyalinized, pale pink stroma (Figure 1B). At low power, the tumor cells were large, eosinophilic and had prominent cytoplasmic vacuoles giving it a sieve-like appearance (Figure 1C). Focal stromal hyalinization (scarring) akin to that seen in RO (Figure 1D),

which was also appreciated in the CT scan (Figure 1A), was seen. The tumor had a nested to tubular architecture with lumen focally filled with pale blue secretions (Figure 1E). At high magnification, the tumor cells exhibited central to eccentric, round nuclei with prominent nucleoli (grade 3) and multinucleation (Figure 1F–H). Focal pleomorphism and degenerative “ancient” change were present. Perinuclear clearing was observed in rare cells and minimal to no nuclear membrane irregularities were seen. Mitosis were not observed. The cells had abundant granular eosinophilic cytoplasm with prominent cell membranes. Psammomatous laminated calcifications were present. A striking feature was the presence of variably sized abundant, often large, cytoplasmic vacuoles (Figure 1H). A few thick-walled abnormal vessels similar to those seen in angiomyolipoma were present within the tumor and especially at the periphery (Figure 1C). No foamy histiocytes, papillary architecture, lymphocytic infiltrate, or aggressive features such as tumor necrosis, vascular invasion or intra-renal parenchymal invasion were observed (and the tumor is quite small). The adjacent renal parenchyma did not show any tumorlets and was largely unremarkable. Mild to moderate atherosclerotic changes were observed consistent with the patient’s history of long-standing hypertension.

Immunohistochemical (IHC) and Electron Microscopy Findings

Immunohistochemically, the tumor cells showed uniform nuclear PAX8, membranous CD117 staining (Figure 2A) and were negative for cytokeratin 7 (Figure 2B). Pankeratin AE1/AE3, CD10, cathepsin-K were patchy positive (Figure 2C and data not shown). To evaluate the status of mTORC1 pathway, we analyzed phospho-S6. Phospho-S6 (Ser240/244) was diffusely positive (Figure 2D). Cytokeratin 20, HMB45, TFEB, TFE3, and CA-IX were all negative. In addition, the tumor cells retained SDHB (succinate dehydrogenase B) and FH (fumarate hydratase) expression.

Electron microscopic (EM) examination (of FFPE tissue post-fixed in glutaraldehyde) revealed numerous mitochondria of normal shape, size, and structure. The cytoplasmic vacuoles seen by light microscopy appeared to correspond to markedly dilated cisterns of rough endoplasmic reticulum (ER) (Figure 2E–F).

Molecular Findings

Representative areas of the primary renal tumor and matched normal tissue were macrodissected for DNA extraction and submitted to BGI Genomics for whole-exome sequencing (WES) after Institutional Review Board (IRB) approval. Sequencing was conducted using a HiSeq2500 (Illumina) to generate 2×75 -bp paired-end reads. The Quantitative Biomedical Research Center (QBRC) mutation calling pipeline (<https://github.com/Somatic-pipeline/Somatic-pipeline>) developed at UT Southwestern Medical Center was used for somatic mutation calling. We carried out somatic copy number variation (CNV) analyses on our exome-seq data using CNVkit (<https://github.com/etal/cnvkit>) with default parameters on tumor-normal pair. Arm gain or loss was called when > 50% of the chromosome exhibited copy number gain or loss⁷.

Whole exome sequencing from tumor and adjacent normal renal parenchyma revealed a somatically acquired *MTOR* mutation (NM_004958.3:c.7280A>T) resulting in a

p.Leu2427Gln substitution (Figure 3A). Variant calls were inspected using Integrated Genomics Viewer (IGV; Figure 3B). Sanger sequencing was performed to validate this mutation (Figure 3C). The mutation appeared to be homo or hemizygous which was consistent with copy number analyses revealing loss of chromosome 1 (likely resulting in loss of remaining wild type *MTOR* gene located on 1p36.22) (Figure 3D). COSMIC and ClinVar were used to annotate the cancer relevance and clinical potential of the detected variant. The mTOR p.L2427Q mutation affects a highly conserved residue in the kinase domain and has been previously reported in several cancer types including RCC and astrocytoma (<https://cancer.sanger.ac.uk/cosmic/mutation/overview?id=105736725>). The mutation is positioned in a unique $\alpha 9b$ insertion specific to mTOR that overlaps with a negative regulatory region whose deletion activates the kinase^{8,9}. The Leu2427 sidechain anchors $\alpha 9b$ alongside the substrate binding groove, linking one end to the FAT helical network (Figure 4A–B). In addition, a mutation of the same residue to a glutamine was identified as the cause of focal cortical dysplasia type II and intractable epilepsy, which is consistent with its increasing mTORC1 activity¹⁰. Furthermore, this same mutation was shown to increase phospho-S6 when ectopically expressed¹⁰. These data suggest that the *MTOR* mutation we identified is activating and while phospho-S6 is often increased in RCC, the strong and diffuse phospho-S6 levels observed are consistent with this notion.

Finally, copy number analyses failed to reveal characteristic chromosomal alterations such as multiple chromosomal losses of chromosome 13, 3p loss in clear cell RCC, or gain of chromosome 7 and 17 as seen in papillary RCC (Figure 3D).

Further Insights into EVT

Our comprehensive analysis of a case of eosinophilic vacuolated tumor (EVT) permits us to leverage the findings to review evolving concepts on this entity. Two recent series reported renal tumors that fit the description of the current case. He et al., described the morphology of 14 cases from multiple institutions and proposed the terminology “high grade oncocyctic tumors (HOT)”⁵. Subsequently, Chen et al., explored the underlying molecular basis using targeted gene sequencing on 5 tumors, identified mutations leading to mTORC1 activation, and proposed the descriptive term of “sporadic renal cell carcinoma with eosinophilic and vacuolated cytoplasm”⁶. A single case has now been reported in a patient with TSC syndrome⁴. Thus, EVT appears to develop in the setting of germline or somatic inactivating mutations of *TSC2* (potentially also *TSC1*) or activating *MTOR* mutations. Similar to our case, most of the tumors reported are small (1.5–7.0 cm; mean 3.4 cm) with no documented aggressive behavior. Though the data are limited, the term “eosinophilic vacuolated tumor” has been preferred over “renal cell carcinoma”. Given the unique morphology that does not fit any of the previously described renal entities, EVT has been proposed by the Genitourinary Pathology Society (GUPS) as one of the emerging new renal tumor entities¹¹.

A number of recently described entities have in common mutations in mTORC1 pathway (*TSC1/TSC2/MTOR/RHEB*). These include EVT, ESC RCC, LOT, and RCC with fibromyxomatous stroma. Renal tumors with similar morphologies are also observed in patients with TSC, who can exhibit a spectrum of additional RCC morphologies. It is currently unclear whether these tumors are related. This is of particular interest given the

recent study that found ChrRCC with mTORC1 pathway mutations to be associated with worse clinical outcomes¹². Mutations in mTORC1 pathway, a key regulator of cell growth and metabolism, have been described in several cancers including traditional subtypes of RCC¹³. Moreover, the morphologic and IHC profiles of these entities are distinct. In everyday practice, morphology remains key and these entities can be recognized prospectively. Separate classification as these entities will enable deeper understanding of their biology, paving the ground for new discoveries in “overlooked genomic studies” and improved disease management. Moreover, recognition of these entities may help initiate investigation for hereditary association and proband genetic testing. Our case illustrates how recognition of these tumors can help better understand their biology by applying state-of-art techniques.

Our study, describes the novel EM and imaging findings of this emerging entity. Markedly dilated cisterns of rough endoplasmic reticulum were noted that corresponded to the cytoplasmic vacuoles seen by light microscopy. Interestingly, this may contribute to explain the increase in phospho-S6 observed in these tumors, as S6 is a ribosomal protein and ribosomes may be increased with the ER expansion. mTORC1 is best known for its role in promoting protein translation, and the ER expansion may contribute to this process¹⁴.

The characteristic association of loss of chromosome 1 along with activating *MTOR* mutations in these tumors is interesting. The findings in our case are similar to the 2 cases reported by Chen et al⁶, with mTOR p.L2427R mutations and chromosome 1 loss. While the reason for chromosome 1 loss is unknown, we speculate that it may be related to mTORC1 being a dimer¹⁵ and that a heterodimer of wild-type and mTOR p.L2427R proteins may not confer sufficient mTORC1 activation.

We have previously published a comprehensive genomic analysis of non-clear cell RCC comparing RO, renal oncocytic neoplasm, and ChrRCC¹⁶. We found that the majority of eosinophilic variant ChrRCC (ChrRCC-eo) lack characteristic DNA copy number alterations seen in classic ChrRCC. ChrRCC-eo have also been shown to harbor somatic mTORC1 pathway alterations¹⁷ and RO have been noted to show partial or complete loss of chromosome 1¹⁸. EVT are morphologically distinct from RO and ChrRCC-eo. They can be distinguished from RO by the presence of nuclear pleomorphism, cell size variation, large cytoplasmic vacuoles and strong diffuse expression of phospho-S6 and cathepsin K^{3,6}. They are dissimilar to ChrRCC-eo in the lack of perinuclear clearing and wrinkled nuclear membranes and the presence of striking cytoplasmic vacuoles (Table 1). EVT also share features with the newly recognized entity of ESC RCCs that are also associated with *TSC1/2* or *MTOR* alterations and like EVT have been described in both the familial and sporadic settings. Unlike EVT, ESC RCCs are more cystic, have cytoplasmic stippling/granularity, lack cytoplasmic vacuolation, and have a different IHC profile (CD117-/vimentin+/CD20+). Like ESC RCC, EVT have high-grade nuclear cytology but no cases with metastasis have been reported as yet². TFEB rearranged RCC can show oncocytic architecture and cathepsin K reactivity, however, nuclear TFEB protein expression by IHC or TFEB break-apart FISH assay can establish the correct diagnosis. In addition, recent studies have reported other eosinophilic renal tumors with a spectrum of overlapping morphology and *TSC1/2* or *MTOR* mutations¹⁹.

In summary, EVT have a unique morphology, IHC, and molecular profile. Recognition of the characteristics of this novel but rare entity will allow for better classification of renal tumors.

Funding Sources:

This work was supported by the NIH sponsored Kidney Cancer SPORE grant (P50CA196516) and endowment from Brock Fund for Medical Science Chair in Pathology and Jan and Bob Pickens Distinguished Professorship in Medical Science.

References

- McKenney JK, Przybycin CG, Trpkov K, Magi-Galluzzi C. Eosinophilic solid and cystic renal cell carcinomas have metastatic potential. *Histopathology*. 2018;72(6):1066–1067. [PubMed: 29265482]
- Trpkov K, Hes O, Bonert M, et al. Eosinophilic, Solid, and Cystic Renal Cell Carcinoma: Clinicopathologic Study of 16 Unique, Sporadic Neoplasms Occurring in Women. *Am J Surg Pathol*. 2016;40(1):60–71. [PubMed: 26414221]
- Siadat F, Trpkov K. ESC, ALK, HOT and LOT: Three Letter Acronyms of Emerging Renal Entities Knocking on the Door of the WHO Classification. *Cancers (Basel)*. 2020;12(1).
- Trpkov K, Bonert M, Gao Y, et al. High-grade oncocytic tumour (HOT) of kidney in a patient with tuberous sclerosis complex. *Histopathology*. 2019;75(3):440–442. [PubMed: 31002177]
- He H, Trpkov K, Martinek P, et al. “High-grade oncocytic renal tumor”: morphologic, immunohistochemical, and molecular genetic study of 14 cases. *Virchows Arch*. 2018;473(6):725–738. [PubMed: 30232607]
- Chen YB, Mirsadraei L, Jayakumaran G, et al. Somatic Mutations of TSC2 or MTOR Characterize a Morphologically Distinct Subset of Sporadic Renal Cell Carcinoma With Eosinophilic and Vacuolated Cytoplasm. *Am J Surg Pathol*. 2019;43(1):121–131. [PubMed: 30303819]
- Talevich E, Shain AH, Botton T, Bastian BC. CNVkit: Genome-Wide Copy Number Detection and Visualization from Targeted DNA Sequencing. *PLoS Comput Biol*. 2016;12(4):e1004873. [PubMed: 27100738]
- Yang H, Rudge DG, Koos JD, Vaidialingam B, Yang HJ, Pavletich NP. mTOR kinase structure, mechanism and regulation. *Nature*. 2013;497(7448):217–223. [PubMed: 23636326]
- Yang H, Jiang X, Li B, et al. Mechanisms of mTORC1 activation by RHEB and inhibition by PRAS40. *Nature*. 2017;552(7685):368–373. [PubMed: 29236692]
- Lim JS, Kim WI, Kang HC, et al. Brain somatic mutations in MTOR cause focal cortical dysplasia type II leading to intractable epilepsy. *Nat Med*. 2015;21(4):395–400. [PubMed: 25799227]
- Trpkov K, Williamson SR, Gill AJ, et al. Novel, emerging and provisional renal entities: The Genitourinary Pathology Society (GUPS) update on renal neoplasia. *Mod Pathol*. 2021.
- Roldan-Romero JM, Santos M, Lanillos J, et al. Molecular characterization of chromophobe renal cell carcinoma reveals mTOR pathway alterations in patients with poor outcome. *Mod Pathol*. 2020;33(12):2580–2590. [PubMed: 32616874]
- Linehan WM, Ricketts CJ. The Cancer Genome Atlas of renal cell carcinoma: findings and clinical implications. *Nat Rev Urol*. 2019;16(9):539–552. [PubMed: 31278395]
- Saxton RA, Sabatini DM. mTOR Signaling in Growth, Metabolism, and Disease. *Cell*. 2017;168(6):960–976. [PubMed: 28283069]
- Aylett CH, Sauer E, Imseng S, et al. Architecture of human mTOR complex 1. *Science*. 2016;351(6268):48–52. [PubMed: 26678875]
- Durinck S, Stawiski EW, Pavia-Jimenez A, et al. Spectrum of diverse genomic alterations define non-clear cell renal carcinoma subtypes. *Nat Genet*. 2015;47(1):13–21. [PubMed: 25401301]
- Davis CF, Ricketts CJ, Wang M, et al. The somatic genomic landscape of chromophobe renal cell carcinoma. *Cancer Cell*. 2014;26(3):319–330. [PubMed: 25155756]

18. Anderson CB, Lipsky M, Nandula SV, et al. Cytogenetic analysis of 130 renal oncocytomas identify three distinct and mutually exclusive diagnostic classes of chromosome aberrations. *Genes Chromosomes Cancer*. 2019.
19. Tjota M, Chen H, Parilla M, Wanjari P, Segal J, Antic T. Eosinophilic Renal Cell Tumors With a TSC and MTOR Gene Mutations Are Morphologically and Immunohistochemically Heterogenous: Clinicopathologic and Molecular Study. *Am J Surg Pathol*. 2020;44(7):943–954. [PubMed: 32091432]

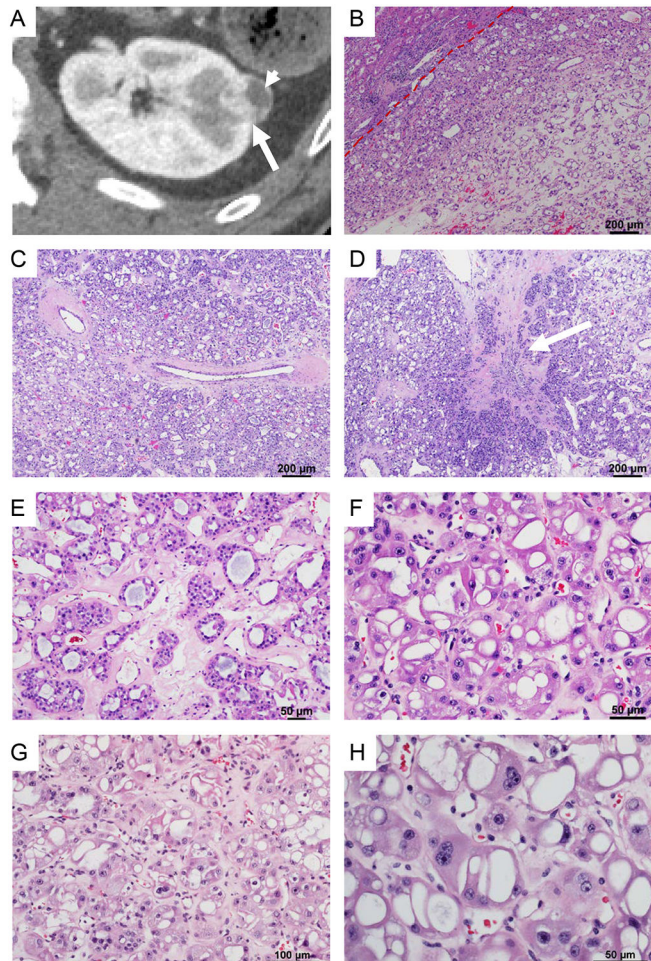


Figure 1. Radiological and microscopic features of Eosinophilic Vacuolated Tumors (EVT). (A) Axial reconstruction of a contrast-enhanced CT acquisition during the corticomedullary phase demonstrating a small renal mass peripherally located in the left kidney. Note disproportionate enhancement (long arrow) suggesting intense angiogenesis. Laterally the mass exhibits an area with decrease enhancement (short arrow). (B) Representative hematoxylin and eosin stained sections reveal a well circumscribed unencapsulated tumor with (C) prominent thick-walled abnormal vessels and (D) focal scarring (white arrow). (E) Tumor cells are arranged in tubular to nested architecture in a hyalinized hypovascular stroma. (F-G) The cells show round nuclei with smooth nuclear membranes, prominent nucleoli, multinucleation and abundant eosinophilic cytoplasmic with distinct cell borders. (H) Characteristic features included the presence of prominent large cytoplasmic vacuoles.

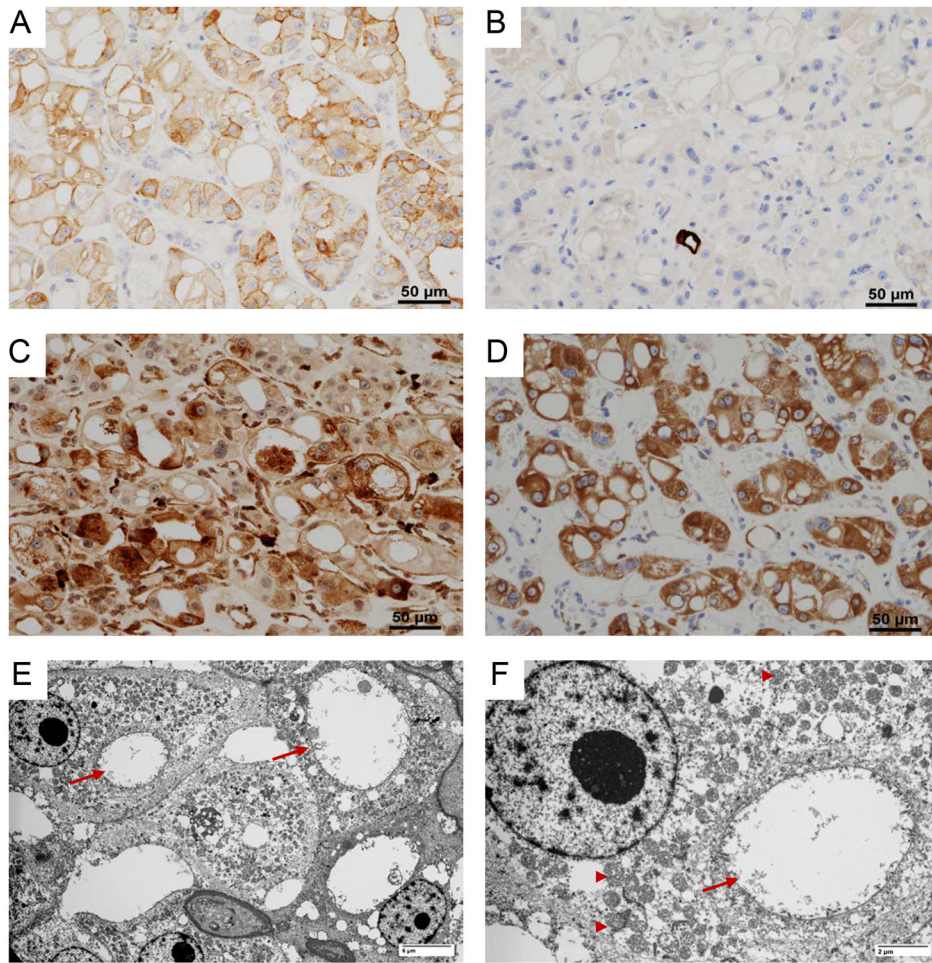


Figure 2. Immunohistochemical features of EVT.

EVT characteristically have (A) positive membranous CD117; (B) negative cyokeratin 7; (C) focal positive cathepsin-K; and (D) diffuse phospho-S6 expression. (E-F) Ultramicrographs showing numerous mitochondria (arrow head) and dilated cisterns of rough endoplasmic reticulum (arrow).

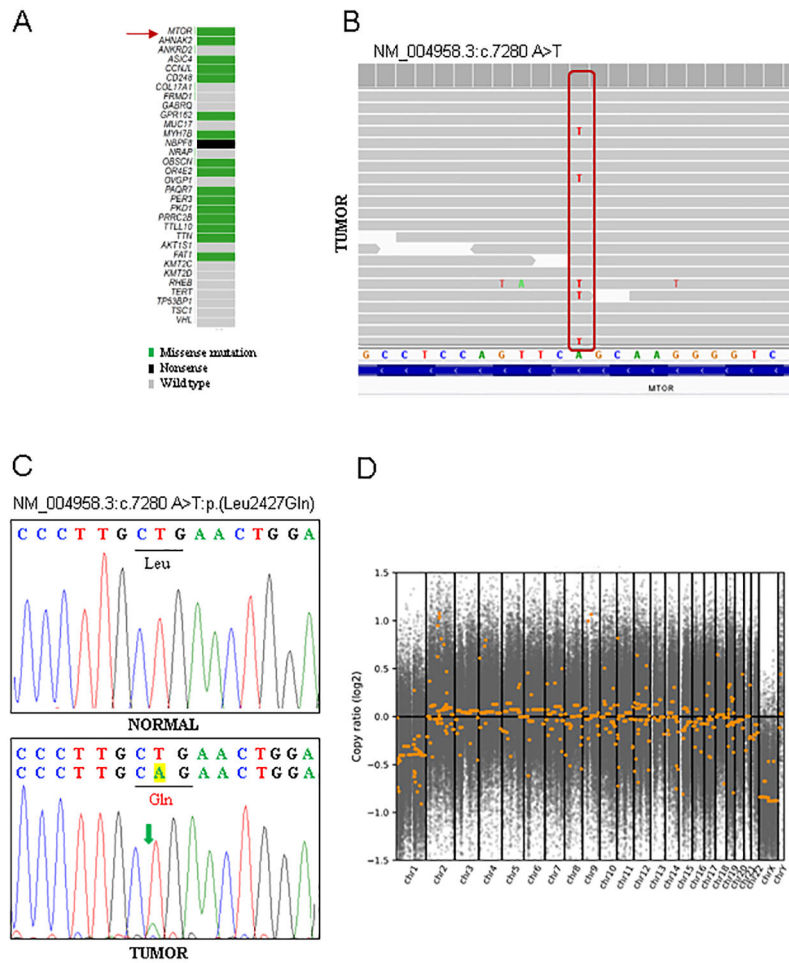


Figure 3. Sequencing analyses.

(A) Oncoplot of selected genes including those with somatic mutations based on COSMIC and (B) screenshot of *MTOR* c.7280A>T mutation viewed with Integrated Genome Viewer (IGV). (C) Sanger sequencing chromatogram validating the mutation. (D) Genome-wide plots showing copy number variation (CNV) analysis of whole exome sequencing with loss of chromosome 1.

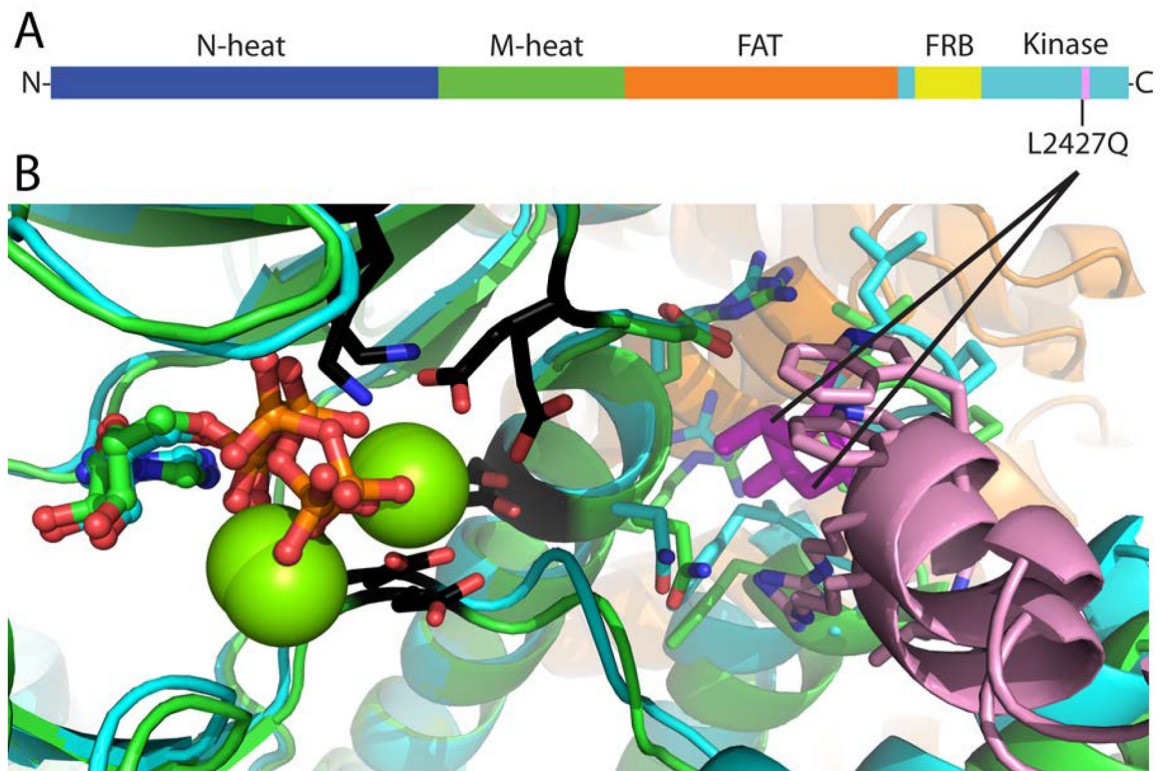


Figure 4. Schematic mapping of mTOR mutations in EVT.

(A) Schematic representation of the mTOR domains along the chain from N-terminus to C-terminus. The position of the L2427Q is indicated. (B) Model showing active (cyan)/inactive (green) kinase domains superimposed, with active site residues in black stick and ATP in ball and stick. The L2427Q mutation is positioned in a unique $\alpha 9b$ insertion (pink) that overlaps with a negative regulatory region whose deletion activates the kinase. The Leu2427 sidechain (magenta stick, with interacting residues within 4 Å in stick) anchors $\alpha 9b$ (pink) alongside the substrate binding groove, linking one end to the FAT helical network (orange).

Table 1.

Synopsis of distinguishing features for the differential diagnosis of EVT.

Entity	Key clinical feature	Key morphologic features	Immunohistochemistry							Molecular Analyses		
			CD117	CK7	CK20	Cathepsin-K	HMB45/Melan A	Vimentin	PAX8	Others	Gene mutations and rearrangement	Frequent Copy number alterations
Eosinophilic vacuolated tumor (EVT)	F>M, small indolent tumors, rare case in TSC patients	solid nest, abundant granular cytoplasm with striking vacuolization, round nuclei with prominent nucleoli	+	-/focal positive	-	+	-	-	+	Phospho S6 +	Diploid, loss of chromosome 1	<i>TSC2</i> , <i>MTOR</i> mutations
Eosinophilic solid and cystic RCC (ESC RCC)	F>M, sporadic, associated with TSC patients, rarely can metastasize	solid and macrocystic architecture, cell with hobnail arrangement in cysts, abundant granular cytoplasm, coarse cytoplasmic stippling, letshmania-like cytoplasmic globules, admixed aggregates of lymphocytes and histiocytes	-	-/focal positive	+	+	-/+	+	Racemase +	Gains of 16p, 16q, 7p, 7q	<i>TSC1</i> , <i>TSC2</i> bi-allelic loss or mutations	
Low-grade oncocytic tumor (LOI)	Older age, small indolent tumors, sporadic, rare case with germline TSC mutations	solid, tight nests of uniform cells with eosinophilic cytoplasm, round nuclei, subtle perinuclear halo, sharply demarcated areas of edematous stroma	-	+++	-	-	-	+		Diploid, loss of 19p, 1p	<i>MTOR</i> , <i>TSC1</i> , <i>RHEB</i> mutations	
Chromophobe RCC, eosinophilic (chRCC, eo)	Sporadic	tight nest/sheet like architecture, purely eosinophilic cytoplasm, prominent cell borders, prominent nuclear membrane irregularities,	+	+/-	-	-	-	+	FOX11 +, LINC01187 +	Diploid, loss of chromosome 1, 2, 6, 10, 13, 17, 21	<i>TP53</i> , <i>PTEN</i> mutations	

Entity	Key clinical feature	Key morphologic features	Immunohistochemistry							Molecular Analyses				
			CD117	CK7	CK20	Cathepsin-K	HMB45/Melan A	Vimentin	PAX8	Others	Gene mutations and rearrangement	Frequent Copy number alterations		
		perinuclear halos, and binucleation												
Epithelioid angiomylipoma (eAML)	Sporadic, associated with TSC syndrome	discohesive high grade, ganglion cell-like epithelioid cells with pleomorphic nuclei	-	-	-	+	+	+					TSC2 mutations, TFE3 rearrangement	
TFEB rearranged RCC (RCC)	Young age	variable architecture, clear and pale fluffy eosinophilic cells, psammoma bodies, biphasic pattern of large and small cells	-	-	-	+/-	+	+					TFEB rearrangement	